
Deep Determinantal Point Processes

Mike Gartrell

Criteo AI Lab

m.gartrell@criteo.com

Elvis Dohmatob

Criteo AI Lab

e.dohmatob@criteo.com

Jon Alberdi

Criteo

j.alberdi@criteo.com

Abstract

Determinantal point processes (DPPs) have attracted significant attention as an elegant model that is able to capture the balance between quality and diversity within sets. DPPs are parameterized by a positive semi-definite kernel matrix. While DPPs have substantial expressive power, they are fundamentally limited by the parameterization of the kernel matrix and their inability to capture nonlinear interactions between items within sets. We present the *deep DPP* model as way to address these limitations, by using a deep feed-forward neural network to learn the kernel matrix. In addition to allowing us to capture nonlinear item interactions, the deep DPP also allows easy incorporation of item metadata into DPP learning. Since the learning target is the DPP kernel matrix, the deep DPP allows us to use existing DPP algorithms for efficient learning, sampling, and prediction. Through an evaluation on several real-world datasets, we show experimentally that the deep DPP can provide a considerable improvement in the predictive performance of DPPs, while also outperforming strong baseline models in many cases.

1 Introduction

Modeling the relationship between items within observed subsets, drawn from a large collection, is an important challenge that is fundamental to many machine learning applications, including recommender systems [13], document summarization [24, 27], and information retrieval [22]. For these applications, we are primarily concerned with selecting a good subset of diverse, high-quality items. Balancing quality and diversity in this setting is challenging, since the number of possible subsets that could be drawn from a collection grows exponentially as the collection size increases.

Determinantal point processes (DPPs) offer an elegant and attractive model for such tasks, since they provide a tractable model that jointly considers set diversity and item quality. A DPP models a distribution over subsets of a ground set \mathcal{Y} that is parametrized by a positive semi-definite matrix $\mathbf{L} \in \mathbb{R}^{|\mathcal{Y}| \times |\mathcal{Y}|}$, such that for any $A \subseteq \mathcal{Y}$,

$$\Pr(A) \propto \det(\mathbf{L}_A), \quad (1)$$

where $\mathbf{L}_A = [\mathbf{L}_{ij}]_{i,j \in A}$ is the submatrix of \mathbf{L} indexed by A . Informally, $\det(\mathbf{L}_A)$ represents the volume associated with subset A , the diagonal entry L_{ii} represents the importance of item i , while entry $L_{ij} = L_{ji}$ encodes the similarity between items i and j . DPPs have been studied in the context of a number of applications [1, 6, 19, 30, 42] in addition to those mentioned above. There has also been significant work regarding the theoretical properties of DPPs [23, 3, 1, 21, 13, 9, 25].

Learning a DPP from observed data in the form of example subsets is a challenging task that is conjectured to be NP-hard [23]. Some work has involved learning a nonparametric full-rank \mathbf{L} matrix [13, 29] that does not constrain \mathbf{L} to take a particular parametric form, while other work has involved learning a low-rank factorization of this nonparametric \mathbf{L} matrix [12, 34]. A low-rank factorization of \mathbf{L} enables substantial improvements in runtime performance compared to a full-rank DPP model during training and when computing predictions, on the order of 10-20x or more, with predictive performance that is equivalent to or better than a full-rank model.

While the low-rank DPP model scales well, it has a fundamental limitation regarding model capacity and expressive power due to the nature of the low-rank factorization of \mathbf{L} . A rank- K factorization of \mathbf{L} has an implicit constraint on the space of possible subsets, since it places zero probability mass on subsets with more than K items. When trained on a dataset containing subsets with at most K items, we observe from the results in [12] that this constraint is reasonable and that the rank- K DPP provides predictive performance that is approximately equivalent to that of the full-rank DPP. Therefore, in this scenario the rank- K DPP can be seen as a good approximation of the full-rank DPP. However, we empirically observe that the rank- K DPP generally does not provide improved predictive performance for values of K greater than the size of the largest subset in the data. Thus, for a dataset containing subsets no larger than size K , from the standpoint of predictive performance, there is generally no utility in increasing the number of low-rank DPP embedding dimensions beyond K , which establishes an upper bound on the capacity of the model. Furthermore, since the determinant is a multilinear function of the columns or rows of a matrix, a DPP is unable to capture nonlinear interactions between items within observed subsets.

The constraints of the standard DPP model motivate us to seek modeling options that enable us to increase the expressive power of the model and improve predictive performance, while still allowing us to leverage the efficient learning, sampling, and prediction algorithms available for DPPs. We present the *deep DPP* as a model that fulfills these requirements. The deep DPP uses a deep feed-forward neural network to learn the low-rank DPP embedding matrix, allowing us to move beyond the constraints of the standard multilinear DPP model by supporting nonlinearities in the embedding space through the use of multiple hidden layers in the deep network. The deep DPP also allows us to incorporate item-level metadata into the model, such as item names, descriptions, etc. Since the learning target of the deep DPP model is the low-rank DPP embedding matrix, we can use existing algorithms for efficient learning, sampling, and prediction for DPPs. Thus, the deep DPP provides us with an elegant deep generative model for sets.

Contributions The main contributions of this work are the following:

- We extend the standard low-rank DPP model by using a deep feed-forward neural network for learning the DPP kernel matrix, which is composed of item embeddings. This approach allows us to arbitrarily increase the expressive power of the deep DPP model by simply adding hidden layers to the deep network.
- The deep DPP supports arbitrary item-level metadata. The deep network in our model allows us to easily incorporate such metadata, and automatically learns parameters that explain how this metadata interacts with the latent item embeddings in our model. In recommendation settings, leveraging metadata has been shown to improve predictive quality [20, 37], particularly for cold-start scenarios with sparse user/item interactions.
- We conduct an extensive experimental evaluation on several real-world datasets. This analysis highlights scenarios in which the deep DPP can provide significantly better predictive quality compared to the standard low-rank DPP. Specifically, we see that the deep DPP is able to extract complex nonlinear item interactions, particularly for large, complex datasets.

2 Related Work

A number of approaches for DPP kernel learning have been studied. [14] presents DPP kernel learning via expectation maximization, while [29] present a fixed-point method. Methods to substantially speed up DPP kernel learning, as compared to learning a full-rank kernel, have leveraged Kronecker [31] and low-rank [10–12, 34] structures. [32] presents methods for incorporating inferred negative samples into the DPP learning task, based on contrastive estimation. Learning guarantees using DPP graph properties are studied in [36].

There has been some prior work regarding the use of a deep neural network to learn DPP model parameters. In [39], the authors describe one approach that involves a deep network, where the model is parameterized in terms of one data instance (an image) for each observed subset of labels. In contrast, our deep DPP model is more general and allows for each item within the ground set \mathcal{Y} to have its own item-level metadata features (item price, description, image, etc.). [38] present an approach for generating YouTube video recommendations, where two different deep networks are used to learn a decomposition of the DPP \mathbf{L} matrix based on item quality scores and item embedding vectors. Our

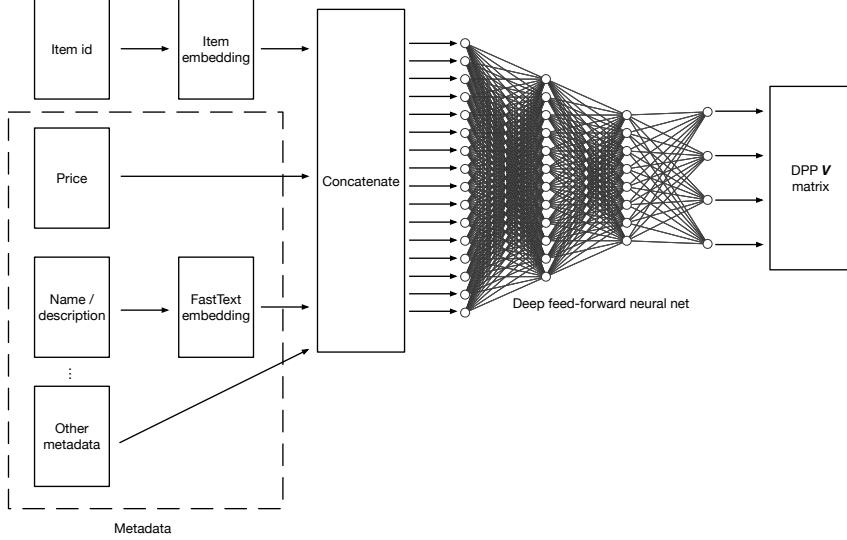


Figure 1: Deep DPP architecture. Observed subsets composed of item ids, as well as optional item-level metadata, are provided as inputs to the deep neural network during learning. The output is the learned $|\mathcal{Y}| \times K$ DPP parameter matrix \mathbf{V} , where each row of this matrix is an item embedding vector.

deep DPP approach differs, in that we implement end-to-end learning of a fully non-parametric \mathbf{L} that does not impose any particular parametric form. [33] presents a deep generative model that efficiently generates samples which approximate samples drawn from a DPP. However, this approach does not involve using a deep network to learn DPP model parameters.

Matrix factorization models are commonly used to model user-item interactions in recommender systems. Although DPP and matrix factorization models are fundamentally different, they are both limited to capturing linear interactions between items or users and items, respectively. An approach to extending the conventional matrix factorization model by using a deep network to learn representations of user and items within a nonlinear embedding space is described in [40]. This deep matrix factorization model bears some conceptual similarity with our deep DPP model, in that both approaches involve extending linear models to accommodate nonlinear interactions by using deep networks.

[8] describes a YouTube recommendation system that uses deep networks for candidate generation and ranking. Features such as user age and gender are concatenated with embeddings for users' watch and search histories to form the first layer of the deep network used for the candidate generation model, and each hidden layer is fully connected. This network architecture bears some similarity to the architecture we use to support both item embeddings and metadata in our deep DPP model, as described in Section 3.

3 Model

We begin this section with some background on DPPs and low-rank DPPs, followed by a discussion of the architecture of our deep DPP model.

Since the normalization constant for Eq. 1 follows from the observation that $\sum_{A \subseteq \mathcal{Y}} \det(\mathbf{L}_A) = \det(\mathbf{L} + \mathbf{I})$, we have

$$\mathcal{P}(A) = \frac{\det(\mathbf{L}_A)}{\det(\mathbf{L} + \mathbf{I})} \quad (2)$$

where a discrete DPP is a probability measure \mathcal{P} on $2^{\mathcal{Y}}$ (the power set or set of all subsets of \mathcal{Y}). Therefore, the probability $\mathcal{P}(A)$ for any $A \subseteq \mathcal{Y}$ is given by Eq. 2.

We use a low-rank factorization of the $|\mathcal{Y}| \times |\mathcal{Y}|$ \mathbf{L} matrix, $\mathbf{L} = \mathbf{V}\mathbf{V}^T$, where $\mathbf{V} \in \mathbb{R}^{|\mathcal{Y}| \times K}$, and $K \leq |\mathcal{Y}|$ is the rank of the kernel. K is fixed *a priori*, and is often set to the size of the largest observed subset in the data.

Algorithm 1 Learning the deep DPP \mathbf{V} matrix

Input: Samples of training subsets \mathcal{A} , initial parameter matrix \mathbf{V}_0 , maxIter, deepNetArch.

BUILDDEEPNET(deepNetArch, \mathbf{V})
 $k \leftarrow 1$
while $k < \text{maxIter}$ **and** not converged **do**
 Compute embeddings matrix \mathbf{V}_k via forward pass
 Sample mini-batch of baskets and evaluate loss $f(\mathbf{V}_k, \mathcal{A})$
 $\mathbf{V}_{k+1} \leftarrow \text{Backprop}$ on loss
end while
return \mathbf{V}_k

Given a collection of N observed subsets $\mathcal{A} = \{A_1, \dots, A_N\}$ composed of items from \mathcal{Y} , our learning task is to fit a DPP kernel \mathbf{L} based on this data. Our training data is these observed subsets \mathcal{A} , and our task is to maximize the likelihood for samples drawn from the same distribution as \mathcal{A} . The log-likelihood for seeing \mathcal{A} is

$$f(\mathbf{V}) = \log \mathcal{P}(\mathcal{A}|\mathbf{V}) = \sum_{n=1}^N \log \mathcal{P}(A_n|\mathbf{V}) = \sum_{n=1}^N \log \det(\mathbf{L}_{[n]}) - N \log \det(\mathbf{L} + \mathbf{I})$$

where $[n]$ indexes the observed subsets in \mathcal{A} .

As described in [12], we augment $f(\mathbf{V})$ with a regularization term:

$$f(\mathbf{V}) = \sum_{n=1}^N \log \det(\mathbf{L}_{[n]}) - N \log \det(\mathbf{L} + \mathbf{I}) - \alpha \sum_{i=1}^{|\mathcal{Y}|} \frac{1}{\lambda_i} \|\mathbf{v}_i\|_2^2 \quad (3)$$

where λ_i counts the number of occurrences of item i in the training set, \mathbf{v}_i is the corresponding row vector of \mathbf{V} , and $\alpha > 0$ is a tunable hyperparameter. This regularization term reduces the magnitude of $\|\mathbf{v}_i\|_2$, which can be interpreted as the popularity of item i , according to its empirical popularity λ_i .

Figure 1 shows the architecture of the deep DPP model. As shown in this figure, a deep network is used to learn \mathbf{V} . Furthermore, this architecture allows us to seamlessly incorporate item metadata, such as price and item name and description, into the model. As shown in Figure 1, we use FastText embeddings [2] to support text-based metadata, such as item names and descriptions. We use self-normalizing SELU activation functions [18] for our deep network, since we empirically found that this activation function provides stable convergence behavior during training. The network is structured according to a common tower-like pattern, where the first layer is widest, and each of the following hidden layers reduces the number of hidden units, until we reach the target embedding size K . For example, a network with three hidden layers for a model for a catalog of 50,000 items and a target embedding size of $K = 100$, not considering metadata, would use the following architecture: $50,000 \rightarrow 400 \rightarrow \text{SELU} \rightarrow 300 \rightarrow \text{SELU} \rightarrow 200 \rightarrow \text{SELU} \rightarrow 100$.

We use the Adam stochastic optimization algorithm [17] to train our model, in conjunction with Hogwild [35] for asynchronous parallel updates during training. Algorithm 1 shows the learning algorithm for our model. All code is implemented in PyTorch¹, and will be made publicly available at a later date.

4 Experiments

We run extensive experiments on several real-world datasets composed of shopping baskets. The primary prediction task we evaluate is next-item prediction, which involves identifying the best item to add to a subset of chosen objects (e.g., basket completion); see Appendix A for details on how we efficiently compute such predictions for the low-rank DPP and deep DPP models. We compare our deep DPP model to the following competing approaches:

1. **Low-rank DPP:** The standard low-rank DPP model [12].

¹<https://pytorch.org>

2. **Poisson Factorization (PF):** Poisson factorization (PF) is a prominent variant of matrix factorization, designed specifically for implicit ratings (e.g., clicks or purchase events) [15]. Since PF is parameterized in terms of users and items, rather than subsets, we train PF by treating each observed basket as a "user". When computing next-item predictions for baskets, inspired by the approach for set expansion described in [41], we average the embeddings for each item within the observed basket; let us denote the resulting embedding vector for the basket as s_A . Then, we compute the unnormalized probability of each possible next item for the basket, which is proportional to the inner product between s_A and the embedding for the next item. We use a publicly available implementation of PF², with default hyperparameter settings, and 30 embedding dimensions.

3. **Low-rank DPP constructed from pre-trained PF embeddings:** We examine the value of end-to-end learning of the deep DPP kernel, compared to a low-rank DPP kernel directly constructed from embeddings learned using a different model. Here, we simply set the low-rank DPP V matrix to the matrix of item embeddings obtained from the PF model, rather than learning the V matrix using the DPP log-likelihood (Eq. 3). We refer to this model as the "pre-trained Poisson" model in Figures 2 and 3.

4.1 Datasets

We perform next-item prediction and AUC-based classification experiments on several real-world datasets composed of purchased shopping baskets:

1. **UK Retail:** This is a public dataset [7] that contains 25,898 baskets drawn from a catalog of 4,070 items, and provides price and description metadata for each item, which we use in our experiments. This dataset contains transactions from a non-store online retail company that primarily sells unique all-occasion gifts, and many customers are wholesalers. We omit all baskets with more than 100 items, which allows us to use a low-rank factorization of the DPP ($K = 100$) that scales well in training and prediction time, while also keeping memory consumption for model parameters to a manageable level.

2. **Belgian Retail Supermarket:** This public dataset³ includes 88,163 baskets, with a catalog consisting of 16,470 unique supermarket items. This dataset was collected in a Belgian retail supermarket over three non-consecutive time periods [5, 4]. We set $K = 100$ for all DPP models trained on this dataset, to accommodate the largest basket found in this dataset.

3. **Instacart:** This public dataset⁴ is composed of 3.2 million baskets purchased by more than 200,000 users of the Instacart service, drawn from a catalog of 49,677 products. We use metadata provided by this dataset that includes supermarket department ID, aisle ID, and product name for each product in our experiments. As with the UK retail dataset, we omit all baskets with more than 100 items. In addition to running experiments on the full dataset, we run experiments on a random sample of 10,000 baskets from the full dataset, with a catalog of 16,258 products for this random sample; we denote this smaller dataset as *Instacart-10k* in the presentation of our experimental results in this paper, while the full dataset is denoted as *Instacart*.

4.2 Experimental setup and metrics

We compare the performance of all methods using a standard recommender system metric: mean percentile rank (MPR).

We begin our definition of MPR by defining percentile rank (PR). First, given a set A , let $p_{i,A} = \Pr(A \cup \{i\} \mid A)$. The percentile rank of an item i given a set A is defined as

$$\text{PR}_{i,A} = \frac{\sum_{i' \notin A} \mathbb{1}(p_{i,A} \geq p_{i',A})}{|\mathcal{Y} \setminus A|} \times 100\%$$

where $\mathcal{Y} \setminus A$ indicates those elements in the ground set \mathcal{Y} that are not found in A .

MPR is then computed as

$$\text{MPR} = \frac{1}{|\mathcal{T}|} \sum_{A \in \mathcal{T}} \text{PR}_{i,A \setminus \{i\}}$$

²<https://github.com/david-cortes/hpfrec>

³<http://fimi.ua.ac.be/data/retail.pdf>

⁴<https://www.instacart.com/datasets/grocery-shopping-2017>

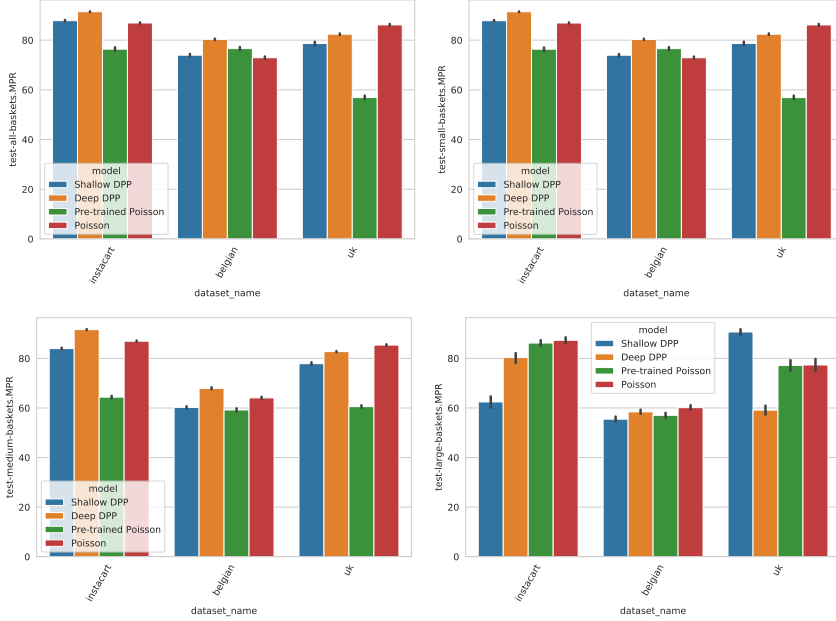


Figure 2: MPR results for the Instacart, Belgian, and UK datasets. Metadata is not used for any of these models.

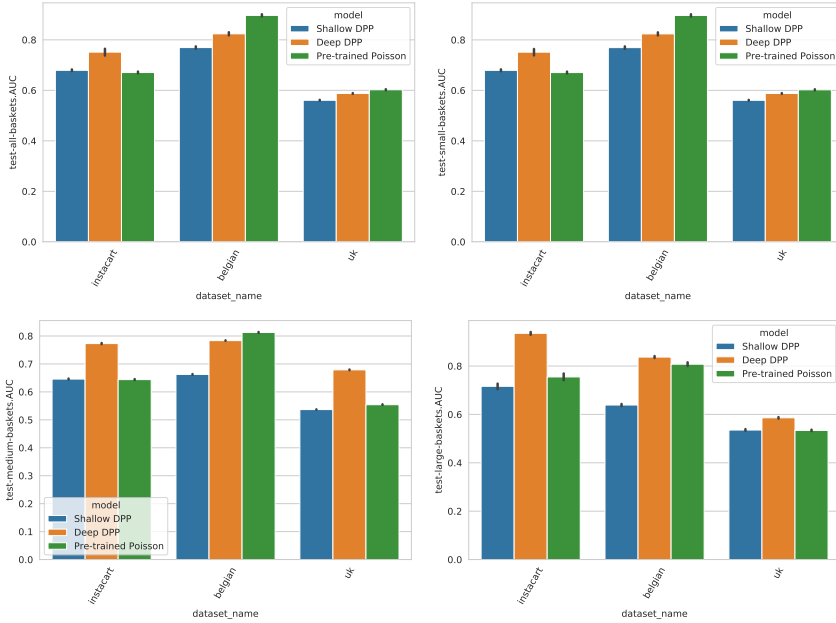


Figure 3: AUC results for the Instacart, Belgian, and UK datasets. Metadata is not used for any of these models.

where \mathcal{T} is the set of test instances and i is a randomly selected element in each set A . A MPR of 50 is equivalent to random selection; a MPR of 100 indicates that the model perfectly predicts the held out item. MPR is a recall-based metric which we use to evaluate the model’s predictive power by measuring how well it predicts the next item in a basket; it is a standard choice for recommender systems [16, 26].

We evaluate the discriminative power of each model using the AUC metric. For this task, we generate a set of negative subsets uniformly at random. For each positive subset A^+ in the test set, we generate a negative subset A^- of the same length by drawing $|A^+|$ samples uniformly at random, and ensure that the same item is not drawn more than once for a subset. We compute the AUC for the model on these positive and negative subsets, where the score for each subset is the log-likelihood that the

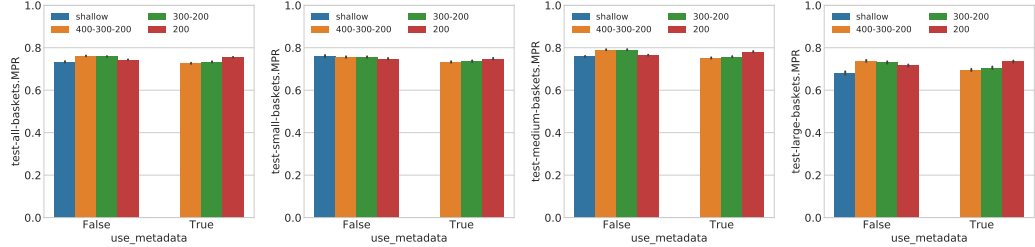


Figure 4: Instacart-10k MPR results, for shallow DPP and deep DPP models trained with and without metadata. We show results for the shallow DPP model (the standard DPP, with no hidden layers), and for deep DPP models with one, two, and three hidden layers, denoted as 200, 300-200, and 400-300-200 hidden layer configurations, respectively.

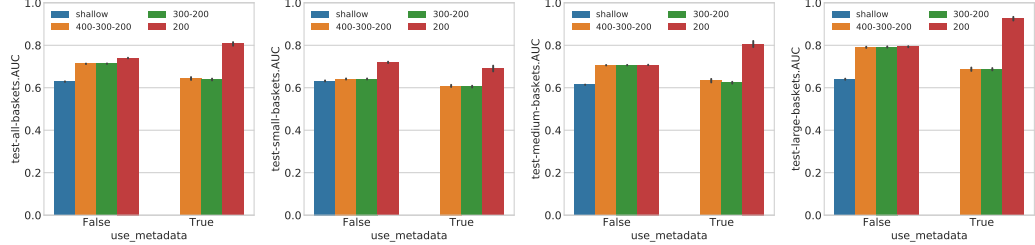


Figure 5: Instacart-10k AUC results, for shallow DPP and deep DPP models trained with and without metadata. We show results for the shallow DPP model (the standard DPP, with no hidden layers), and for deep DPP models with one, two, and three hidden layers, denoted as 200, 300-200, and 400-300-200 hidden layer configurations, respectively.

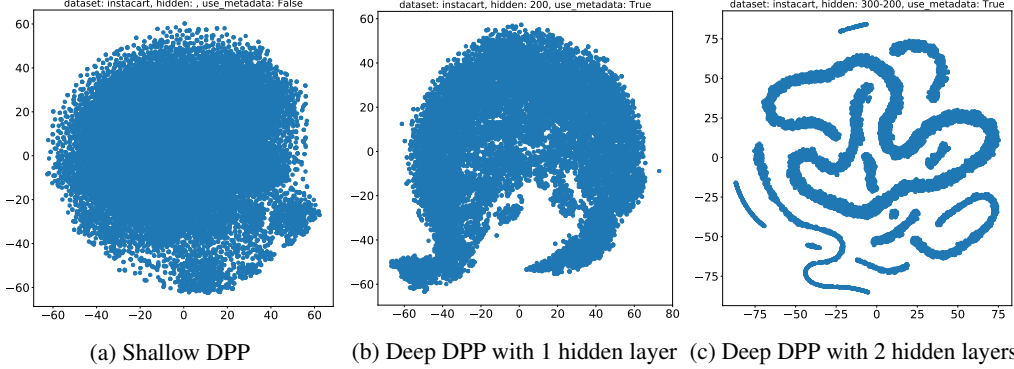


Figure 6: t-SNE plots of product embeddings for the Instacart-10k dataset, for the shallow DPP (with no hidden layers), deep DPP with one hidden layer, and deep DPP with two hidden layers. The deep DPP models are trained with metadata, while the shallow DPP does not support metadata.

model assigns to the subset. This task measures the ability of the model to discriminate between observed positive subsets (ground-truth subsets) and randomly generated subsets.

For all experiments, a random selection of 2000 baskets are used for testing, a random selection of 300 baskets are used for the validation set for tuning hyperparameters and tracking convergence, and the remaining baskets in the dataset are used for training. Convergence is reached during training when the relative change in validation log-likelihood is below a pre-determined threshold, which is set identically for all models; or after training for a maximum of 1000 iterations. We set $\alpha = 1$ for the standard low-rank DPP baseline model, which we found to be a reasonably optimal value for all datasets used in our evaluation, in line with prior work [12]. We set $\alpha = 0$ for the deep DPP models, which we found to be reasonably optimal for all datasets and model configurations.

4.3 Results

Figures 2 through 5 show the results of our experiments; these plots show mean and 95% confidence interval estimates (as error bars) for the MPR and AUC metrics obtained using bootstrapping. For Figures 2 and 3, we select optimal deep DPP model configuration across the results for deep DPPs

with one, two, and three hidden layers. The results for the shallow model in these figures refers to the standard low-rank DPP model, with 0 hidden layers. In addition to computing our results on all test baskets, we also computed results on the test set divided into three equally-sized populations segmented according to basket size.

Figure 2 shows the MPR results for our experiments. Compared to the best performing baseline models, we see that the deep DPP model leads to larger MPR improvements for the Instacart and Belgian datasets than for the UK dataset (where the PF model performs best). The Instacart and Belgian datasets are of higher complexity than the UK datasets, so the larger improvement in MPR for these two datasets suggests that the deep DPP is able to effectively capture the additional signal available in higher complexity datasets. The deep DPP substantially outperforms the pre-trained DPP ("pre-trained Poisson") in most cases, indicating the value of end-to-end learning of the deep DPP kernel as compared to building the kernel from pre-trained embeddings obtained from another model.

Figure 3 shows the AUC results for our experiments. We see that the deep DPP model provides moderate to large AUC improvements for the Instacart, Belgian, and UK datasets over the standard low-rank DPP. Compared to the low-rank DPP, the deep DPP is above to provide somewhat larger AUC improvements for the Instacart and Belgian datasets than for the UK dataset, again suggesting that the deep DPP is able capture the additional complexity in interaction among items in higher complexity datasets. Overall, these results suggest that the using a deep network to learn the DPP kernel is effective at improving the discriminative power of DPPs, particularly for more complex datasets. We see that the deep DPP matches or outperforms the pre-trained DPP in most cases (expect for the Belgian dataset), providing further evidence of the value of end-to-end learning of the deep DPP kernel. Note that we cannot use the PF model to assign a score to a subset (basket) in a straightforward manner, and so we omit the PF model from this analysis.

To evaluate the impact of training deep DPP models with metadata, figures 4 and 5 show the MPR and AUC results for our experiments on the Instacart-10k dataset, where models are trained with and without the metadata available for this dataset. We use the Instacart-10k dataset for these experiments since it has higher sparsity than the full Instacart dataset, emphasizing the impact of metadata in a high-sparsity setting. The shallow (standard) low-rank DPP is unable to natively support metadata, since this would require manual feature engineering that we have not implemented, and hence results for this model with metadata are not available. From the AUC results, we see that training deep DPP models with metadata is effective at significantly improving the discriminative power of the model. From the MPR results, we see that using metadata generally provides small to moderate improvements in predictive performance. We see somewhat larger MPR improvements for large baskets when using metadata. Since larger baskets are less common in this dataset, this result suggests that metadata can be useful in improving model performance for sparse regions of the data. The substantial AUC improvement of approximately 0.2 for large baskets when using metadata for the best deep model, as compared to the shallow DPP without metadata, is another indication of the improvements that metadata can bring for sparse areas of the data.

t-SNE plots [28] for the item embeddings learned by the deep DPP and standard DPP for the Instacart-10k dataset are shown in Figure 6. We see that the standard shallow DPP learns item embeddings that are approximately distributed within a sphere. For the deep DPP models, we see that as we increase the number of hidden layers, the structure of the embedding space becomes more well defined. These plots suggest that deep DPP models are able to learn complex nonlinear interactions between items.

5 Conclusion

We have introduced the deep DPP model, which uses a deep feed-forward neural network to learn the DPP kernel matrix containing item embeddings. The deep DPP overcomes several limitations of the standard DPP model by allowing us to arbitrary increase the expressive power of the model through capturing nonlinear item interactions, while still leveraging the efficient learning, sampling, and prediction algorithms available for standard DPPs. The deep DPP architecture also allows us to easily incorporate item metadata into DPP learning. Experimentally, we have shown that compared to standard DPPs, which can only capture linear interactions among items, the deep DPP can significantly improve predictive performance, while also improving the model's ability to discriminate between real and randomly generated subsets. Our evaluation also shows that the deep DPP is capable of outperforming strong baseline models in many cases.

References

- [1] R. Affandi, E. Fox, R. Adams, and B. Taskar. Learning the parameters of determinantal point process kernels. In *ICML*, 2014.
- [2] Piotr Bojanowski, Edouard Grave, Armand Joulin, and Tomas Mikolov. Enriching word vectors with subword information. *Transactions of the Association for Computational Linguistics*, 5:135–146, 2017. ISSN 2307-387X.
- [3] Alexei Borodin. Determinantal Point Processes. *arXiv:0911.1153*, 2009.
- [4] Tom Brijs. Retail market basket data set. In *Workshop on Frequent Itemset Mining Implementations (FIMI'03)*, 2003.
- [5] Tom Brijs, Gilbert Swinnen, Koen Vanhoof, and Geert Wets. Using association rules for product assortment decisions: A case study. In *Proceedings of the fifth ACM SIGKDD international conference on Knowledge discovery and data mining*, pages 254–260. ACM, 1999.
- [6] Wei-Lun Chao, Boqing Gong, Kristen Grauman, and Fei Sha. Large-margin determinantal point processes. In *Uncertainty in Artificial Intelligence (UAI)*, 2015.
- [7] D Chen. Data mining for the online retail industry: A case study of rfm model-based customer segmentation using data mining. *Journal of Database Marketing and Customer Strategy Management*, 19(3), August 2012.
- [8] Paul Covington, Jay Adams, and Emre Sargin. Deep neural networks for youtube recommendations. In *RecSys*. ACM, 2016.
- [9] Laurent Decreusefond, Ian Flint, Nicolas Privault, and Giovanni Luca Torrisi. Determinantal Point Processes, 2015.
- [10] Christophe Dupuy and Francis Bach. Learning Determinantal Point Processes in sublinear time, 2016.
- [11] Mike Gartrell, Ulrich Paquet, and Noam Koenigstein. Bayesian low-rank determinantal point processes. In *RecSys*. ACM, 2016.
- [12] Mike Gartrell, Ulrich Paquet, and Noam Koenigstein. Low-rank factorization of Determinantal Point Processes. In *AAAI*, 2017.
- [13] J. Gillenwater. *Approximate Inference for Determinantal Point Processes*. PhD thesis, University of Pennsylvania, 2014.
- [14] J. Gillenwater, A. Kulesza, E. Fox, and B. Taskar. Expectation-maximization for learning Determinantal Point Processes. In *NIPS*, 2014.
- [15] Prem Gopalan, Jake M Hofman, and David M Blei. Scalable recommendation with hierarchical Poisson factorization. In *UAI*, 2015.
- [16] Yifan Hu, Yehuda Koren, and Chris Volinsky. Collaborative filtering for implicit feedback datasets. In *Proceedings of the 2008 Eighth IEEE International Conference on Data Mining*, 2008.
- [17] Diederik P Kingma and Jimmy Ba. Adam: A method for stochastic optimization. In *ICLR*, 2015.
- [18] Günter Klambauer, Thomas Unterthiner, Andreas Mayr, and Sepp Hochreiter. Self-normalizing neural networks. In *NIPS*, 2017.
- [19] Andreas Krause, Ajit Singh, and Carlos Guestrin. Near-optimal sensor placements in Gaussian processes: theory, efficient algorithms and empirical studies. *JMLR*, 9:235–284, 2008.
- [20] Maciej Kula. Metadata embeddings for user and item cold-start recommendations. *arXiv preprint arXiv:1507.08439*, 2015.

- [21] A. Kulesza. *Learning with Determinantal Point Processes*. PhD thesis, University of Pennsylvania, 2013.
- [22] A. Kulesza and B. Taskar. k-dpps: Fixed-size determinantal point processes. In *ICML*, 2011.
- [23] A. Kulesza and B. Taskar. *Determinantal Point Processes for machine learning*, volume 5. Foundations and Trends in Machine Learning, 2012.
- [24] Alex Kulesza and Ben Taskar. Learning determinantal point processes. In *UAI*, 2011.
- [25] Frédéric Lavancier, Jesper Møller, and Ege Rubak. Determinantal Point Process models and statistical inference. *Journal of the Royal Statistical Society: Series B (Statistical Methodology)*, 77(4):853–877, 2015.
- [26] Yanen Li, Jia Hu, ChengXiang Zhai, and Ye Chen. Improving one-class collaborative filtering by incorporating rich user information. In *Proceedings of the 19th ACM International Conference on Information and Knowledge Management*, CIKM ’10, 2010.
- [27] H. Lin and J. Bilmes. Learning mixtures of submodular shells with application to document summarization. In *Uncertainty in Artificial Intelligence (UAI)*, 2012.
- [28] Laurens van der Maaten and Geoffrey Hinton. Visualizing data using t-sne. *Journal of machine learning research*, 9(Nov):2579–2605, 2008.
- [29] Zelda Mariet and Suvrit Sra. Fixed-point algorithms for learning Determinantal Point Processes. In *ICML*, 2015.
- [30] Zelda Mariet and Suvrit Sra. Diversity networks. *Int. Conf. on Learning Representations (ICLR)*, 2016.
- [31] Zelda Mariet and Suvrit Sra. Kronecker Determinantal Point Processes. In *NIPS*, 2016.
- [32] Zelda Mariet, Mike Gartrell, and Suvrit Sra. Learning determinantal point processes by sampling inferred negatives. In *AISTATS, to appear*, 2019.
- [33] Zelda Mariet, Yaniv Ovadia, and Jasper Snoek. Dppnet: Approximating determinantal point processes with deep networks. *arXiv preprint arXiv:1901.02051*, 2019.
- [34] Takayuki Osogami, Rudy Raymond, Akshay Goel, Tomoyuki Shirai, and Takanori Maehara. Dynamic Determinantal Point Processes. In *AAAI*, 2018.
- [35] Benjamin Recht, Christopher Re, Stephen Wright, and Feng Niu. Hogwild: A lock-free approach to parallelizing stochastic gradient descent. In *NIPS*, 2011.
- [36] John Urschel, Victor-Emmanuel Brunel, Ankur Moitra, and Philippe Rigollet. Learning Determinantal Point Processes with moments and cycles. In *Proceedings of the 34th International Conference on Machine Learning, ICML*, pages 3511–3520, 2017.
- [37] Flavian Vasile, Elena Smirnova, and Alexis Conneau. Meta-prod2vec: Product embeddings using side-information for recommendation. In *RecSys*, 2016.
- [38] Mark Wilhelm, Ajith Ramanathan, Alexander Bonomo, Sagar Jain, Ed H Chi, and Jennifer Gillenwater. Practical diversified recommendations on youtube with determinantal point processes. In *CIKM*. ACM, 2018.
- [39] Pengtao Xie, Ruslan Salakhutdinov, Luntian Mou, and Eric P Xing. Deep determinantal point process for large-scale multi-label classification. In *ICCV*, pages 473–482, 2017.
- [40] Hong-Jian Xue, Xinyu Dai, Jianbing Zhang, Shujian Huang, and Jiajun Chen. Deep matrix factorization models for recommender systems. In *IJCAI*, 2017.
- [41] Manzil Zaheer, Satwik Kottur, Siamak Ravanbakhsh, Barnabas Poczos, Ruslan R Salakhutdinov, and Alexander J Smola. Deep sets. In *NIPS*, pages 3391–3401, 2017.
- [42] Cheng Zhang, Hedvig Kjellström, and Stephan Mandt. Stochastic learning on imbalanced data: Determinantal Point Processes for mini-batch diversification. *CoRR*, abs/1705.00607, 2017.

A Computing Predictions

Next-item prediction involves identifying the best item to add to a subset of chosen objects (e.g., basket completion), and is the primary prediction task we evaluate in Section 4. We compute next-item predictions for subsets using the approach for efficient low-rank DPP conditioning described in [32]. As in [13], we first compute the dual kernel $\mathbf{C} = \mathbf{B}^\top \mathbf{B}$, where $\mathbf{B} = \mathbf{V}^\top$. We then compute

$$\mathbf{C}^A = (\mathbf{B}^A)^\top \mathbf{B}^A = \mathbf{Z}^A \mathbf{C} \mathbf{Z}^A,$$

with $\mathbf{Z}^A = \mathbf{I} - \mathbf{B}_A(\mathbf{B}_A^\top \mathbf{B}_A)^{-1} \mathbf{B}_A^\top$, where \mathbf{C}^A is the DPP kernel conditioned on the event that all items in A are observed, and \mathbf{B}_A is the restriction of \mathbf{B} to the rows and columns indexed by A .

Next, as described in [23], we eigendecompose \mathbf{C}^A to compute the conditional (marginal) probability P_i of every possible item i in \bar{A} :

$$P_i = \sum_{n=1}^K \frac{\lambda_n}{\lambda_n + 1} \left(\frac{1}{\sqrt{\lambda_n}} \mathbf{b}_i^A \hat{\mathbf{v}}_n \right)^2$$

where \mathbf{b}_i^A is a column vector for item i in \mathbf{B}^A , $(\lambda_n, \hat{\mathbf{v}}_n)$ are an eigenvalue/vector of \mathbf{C}^A , and $\bar{A} = \mathcal{Y} - A$. As shown in [32], the overall computational complexity for computing next-item conditionals/predictions for the low-rank DPP using this dual kernel approach is $\mathcal{O}(K^3 + |A|^3 + K^2|A|^2 + |\bar{A}|K^2)$. Since in most cases $K \ll |\bar{A}|$, this allows for efficient conditioning that is essentially linear in the size of the catalog.